Chapter 10

Neutrinoless Double Beta Decay

Petr Vogel
Kellogg Radiation Laboratory
Caltech, Pasadena, CA 91125, USA *

10.1. Introduction - fundamentals of $\beta\beta$ decay

In the recent past neutrino oscillation experiments have convincingly shown that neutrinos have a finite mass. However, in oscillation experiments only the differences of squares of the neutrino masses, $\Delta m^2 \equiv |m_2^2 - m_1^2|$, can be measured, and the results do not depend on the charge conjugation properties of neutrinos, i.e., whether they are Dirac or Majorana fermions. Nevertheless, a lower limit on the absolute value of the neutrino mass scale, $m_{scale} = \sqrt{|\Delta m^2|}$, has been established in this way. Its existence, in turn, is causing a renaissance of enthusiasm in the double beta decay community which is expected to reach and even exceed, in the next generation of experiments, the sensitivity corresponding to this mass scale. Below I review the current status of the double beta decay and the effort devoted to reach the required sensitivity, as well as various issues in theory (or phenomenology) concerning the relation of the $0\nu\beta\beta$ decay rate to the absolute neutrino mass scale and to the general problem of the Lepton Number Violation (LNV).

But before doing that I very briefly summarize the achievements of the neutrino oscillation searches and the role that the search for the neutrinoless double beta decay plays in the elucidation of the pattern of neutrino masses and mixing. In these introductory remarks I use the established terminology, some of which will be defined only later in the text.

There is a consensus that the measurement of atmospheric neutrinos by the SuperKamiokande collaboration[?] can be only interpreted as a conse-

*email: pxv@caltech.edu

quence of the nearly maximum mixing between ν_μ and ν_τ neutrinos, with the corresponding mass squared difference $|\Delta m^2_{atm}| \sim 2.4 \times 10^{-3}\text{eV}^2$. This finding was confirmed by the K2K experiment[?] that uses accelerator ν_μ beam pointing towards the SuperKamiokande detector 250 km away, as well as by the very recent first result of the MINOS experiment located at the Sudan mine in Minnesota, 735 km away from the Fermilab.[?] Several large long-baseline experiments are being built to further elucidate this discovery, and determine the corresponding parameters more accurately.

At the same time the "solar neutrino puzzle", which has been with us for over thirty years since the pioneering chlorine experiment of Davis,[?] also reached the stage where the interpretation of the measurements in terms of oscillations between the ν_e and some combination of the active, i.e., ν_μ and ν_τ neutrinos, is inescapable. In particular, the juxtaposition of the results of the SNO experiment[?] and SuperKamiokande,[?] together with the earlier solar neutrino flux determination in the gallium experiments,[?,?] leads to that conclusion. The value of the corresponding oscillation parameters, however, remained uncertain, with several "solutions" possible, although the so-called Large Mixing Angle (LMA) solution with $\sin^2 2\theta_{sol} \sim 0.8$ and $\Delta m^2_{sol} \sim 10^{-4}\text{eV}^2$ was preferred. A decisive confirmation of the "solar" oscillations was provided by the nuclear reactor experiment KamLAND[?,?] that demonstrated that the flux of the reactor $\bar{\nu}_e$ is reduced and its spectrum distorted at the average distance $\sim$ 180 km from nuclear reactors.

The pattern of neutrino mixing is further simplified by the constraint due to the Chooz and Palo Verde reactor neutrino experiments[?,?] which lead to the conclusion that the third mixing angle, θ_{13}, is small, $\sin^2 2\theta_{13} \le 0.1$. The two remaining possible neutrino mass patterns are illustrated in Fig.**??**.

Altogether, clearly a *lower* limit for at least one of the neutrino masses, $\sqrt{\Delta m^2_{atm}} \simeq 0.05$ eV has been established. However, the oscillation experiments cannot determine the absolute magnitude of the masses and, in particular, cannot at this stage separate two rather different scenarios, the hierarchical pattern of neutrino masses in which $m \sim \sqrt{\Delta m^2}$ and the degenerate pattern in which $m \gg \sqrt{\Delta m^2}$. It is hoped that the search for the neutrinoless double beta decay, reviewed here, will help in foreseeable future in determining, or at least narrowing down, the absolute neutrino mass scale, and in deciding which of these two possibilities is applicable.

Moreover, the oscillation results do not tell us anything about the properties of neutrinos under charge conjugation. While the charged leptons are Dirac particles, distinct from their antiparticles, neutrinos may be the ultimate neutral particles, as envisioned by Majorana, that are identical to

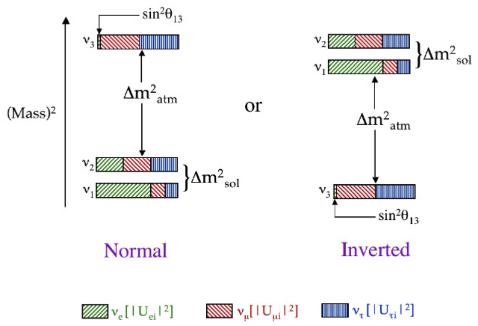

Fig. 10.1. Schematic illustration (mass intervals not to scale) of the decomposition of the neutrino mass eigenstates ν_i in terms of the flavor eigenstates. The two hierarchies cannot be, at this time, distinguished. The small admixture of ν_e into ν_3 is an upper limit.

their antiparticles. That fundamental distinction becomes important only for massive particles and becomes irrelevant in the massless limit. Neutrinoless double beta decay proceeds only when neutrinos are massive Majorana particles, hence its observation would resolve the question.

Double beta decay ($\beta\beta$) is a nuclear transition $(Z, A) \rightarrow (Z + 2, A)$ in which two neutrons bound in a nucleus are simultaneously transformed into two protons plus two electrons (and possibly other light neutral particles). This transition is possible and potentially observable because nuclei with even Z and N are more bound than the odd-odd nuclei with the same $A = N + Z$. Analogous transition of two protons into two neutrons are also, in principle, possible in several nuclei, but phase space considerations give preference to the former mode.

An example is shown in Fig. **??**. The situation shown there is not exceptional. There are eleven analogous cases (candidate nuclei) with the Q-value (i.e., the energy available to leptons) in excess of 2 MeV.

There are two basic modes of the $\beta\beta$ decay. In the two-neutrino mode ($2\nu\beta\beta$) there are two $\bar{\nu}_e$ emitted together with the two e^-. Lepton number is conserved and this mode is allowed in the standard model of electroweak interaction. It has been repeatedly observed by now in a number of cases and proceeds with a typical half-life of $\sim 10^{20}$years. In contrast, in the neutrinoless mode ($0\nu\beta\beta$) only the $2e^-$ are emitted and nothing else. That mode clearly violates the law of lepton number conservation and is forbidden in the standard model. Hence, its observation would be a signal of a "new physics".

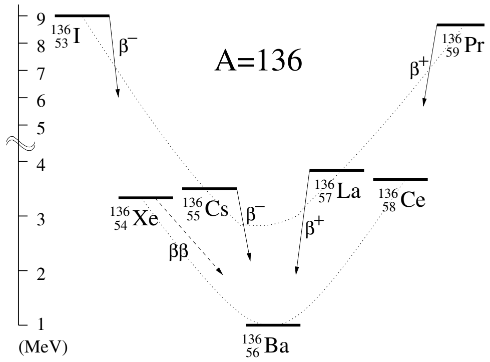

Fig. 10.2. Atomic masses of the isotopes with $A = 136$. Nuclei ^{136}Xe, ^{136}Ba and ^{136}Ce are stable against the ordinary β decay; hence they exist in nature. However, energy conservation alone allows the transition $^{136}\mathrm{Xe} \to {}^{136}\mathrm{Ba} + 2e^-$ (+ possibly other neutral light particles) and the analogous decay of ^{136}Ce with the positron emission.

The two modes of the $\beta\beta$ decay have some common and some distinct features. The common features are:

- The leptons carry essentially all available energy. The nuclear recoil is negligible, $Q/Am_p \ll 1$.
- The transition involves the 0^+ ground state of the initial nucleus and (in almost all cases) the 0^+ ground state of the final nucleus. In few cases the transition to an excited 0^+ state in the final nucleus is energetically possible, but suppressed by the smaller phase space available. (But the $2\nu\beta\beta$ decay to the excited 0^+ state has been observed in few cases.)
- Both processes are of second order of weak interactions, $\sim G_F^4$, hence inherently slow. The phase space consideration alone (for the $2\nu\beta\beta$ mode $\sim Q^{11}$ and for the $0\nu\beta\beta$ mode $\sim Q^5$) give preference to the $0\nu\beta\beta$ which is, however, forbidden by the lepton number conservation.

The distinct features are:

- In the $2\nu\beta\beta$ mode the two neutrons undergoing the transition are uncorrelated (but decay simultaneously) while in the $0\nu\beta\beta$ the two neutrons are correlated.

- In the $2\nu\beta\beta$ mode the sum electron kinetic energy T_1+T_2 spectrum is continuous and peaked below $Q/2$. As $T_1+T_2 \rightarrow Q$ the spectrum approaches zero approximately like $(\Delta E/Q)^6$.
- On the other hand, in the $0\nu\beta\beta$ mode $T_1+T_2=Q$ smeared only by the detector resolution.

These last features allow one to separate the two modes experimentally by observing the sum electron spectrum with a good energy resolution, even if the corresponding decay rate for the $0\nu\beta\beta$ mode is much smaller than for the $2\nu\beta\beta$ mode. This is illustrated in Fig.**??** where the insert that includes the 0ν peak and the 2ν tail shows the situation for the rate ratio of $1:10^6$ corresponding to the most sensitive current experiments.

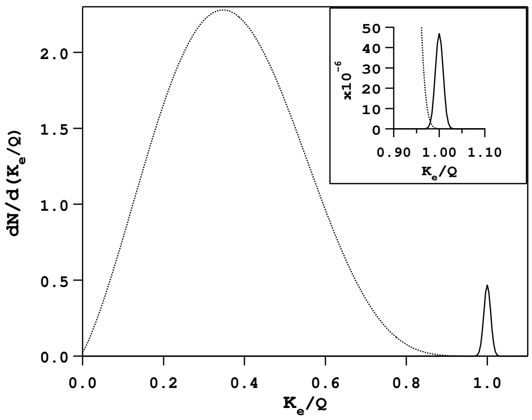

Fig. 10.3. Separating the $0\nu\beta\beta$ mode from the $2\nu\beta\beta$ by the shape of the sum electron spectrum (kinetic energy K_e of the two electrons), including the effect of the 2% resolution smearing. The assumed $2\nu/0\nu$ rate ratio is 10^2, and 10^6 in the insert.

Various aspects, both theoretical and experimental, of the $\beta\beta$ decay have been reviewed many times. Here I quote just the more recent review articles,[?,?,?,?] earlier references can be found there.

In this introductory section let me make only few general remarks. The existence of the $0\nu\beta\beta$ decay would mean that on the elementary particle level a six fermion lepton number violating amplitude transforming two u quarks into two d quarks and two electrons is nonvanishing. As was first pointed out by Schechter and Valle[?] more than twenty years ago, this fact alone would guarantee that neutrinos are massive Majorana fermions (see Fig.**??**). This qualitative statement (or theorem), unfortunately, does not allow us to deduce the magnitude of the neutrino mass once the rate of the $0\nu\beta\beta$ decay have been determined.

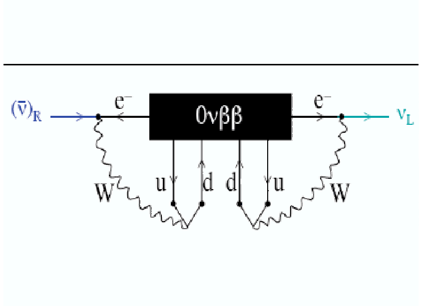

Fig. 10.4. By adding loops involving only standard weak interaction processes the $0\nu\beta\beta$ decay amplitude (the black box) implies the existence of the Majorana neutrino mass.

There is no indication at the present time that neutrinos have nonstandard interactions, i.e. they seem to have only interactions carried by the W and Z bosons that are contained in the Standard Electroweak Model. All observed oscillation phenomena can be understood if one assumes that that neutrinos interact exactly the way the Standard Model prescribes, but are massive fermions forcing a generalization of the model. If we accept this, but in addition assume that neutrinos are Majorana particles, we can in fact relate the $0\nu\beta\beta$ decay rate to the quantity related to the absolute neutrino mass. With these caveats that relation can be expressed as

$$\frac{1}{T_{1/2}^{0\nu}} = G^{0\nu}(Q,Z)|M^{0\nu}|^2 \langle m_{\beta\beta} \rangle^2 \ , \tag{10.1}$$

where $G^{0\nu}(Q,Z)$ is a phase space factor that depends on the transition Q value and through the Coulomb effect on the emitted electrons on the nuclear charge Z and that can be easily and accurately calculated, $M^{0\nu}$ is the nuclear matrix element that can be evaluated in principle, although with a considerable uncertainty, and finally the quantity $\langle m_{\beta\beta} \rangle$ is the effective neutrino Majorana mass, representing the important particle physics ingredient of the process.

In turn, the effective mass $\langle m_{\beta\beta} \rangle$ is related to the mixing angles θ_{ij} that are determined or constrained by the oscillation experiments, to the absolute neutrino masses m_i of the mass eigenstates ν_i and to the as of now totally unknown additional parameters as fundamental as the mixing angles θ_{ij}, the so-called Majorana phase $\alpha(i)$,

$$\langle m_{\beta\beta} \rangle = |\Sigma_i |U_{ei}|^2 e^{i\alpha(i)} m_i| \ . \tag{10.2}$$

Here U_{ei} are the matrix elements of the first row of the neutrino mixing matrix.

It is straightforward to use the eq.(**??**) and the known neutrino oscillation results in order to relate $\langle m_{\beta\beta} \rangle$ to other neutrino mass dependent quantities. This is illustrated in Fig.**??**. Traditionally such plot is made as in the left panel. However, the lightest neutrino mass m_{min} is not an observable quantity. For that reason the other two panels show the relation of $\langle m_{\beta\beta} \rangle$ to the sum of the neutrino masses $M = \Sigma m_i$ and also to $\langle m_\beta \rangle$ that represents the parameter that can be determined or constrained in ordinary β decay,

$$\langle m_\beta \rangle^2 = \Sigma_i |U_{ei}|^2 m_i^2 \ . \tag{10.3}$$

Several remarks are in order. First, the observation of the $0\nu\beta\beta$ decay and determination of $\langle m_{\beta\beta} \rangle$, even when combined with the knowledge of M and/or $\langle m_\beta \rangle$ does not allow, in general, to distinguish between the normal and inverted mass orderings. This is a consequence of the fact that the Majorana phases are unknown. In regions in Fig. **??** where the two hatched bands overlap it is clear that two solutions with the same $\langle m_{\beta\beta} \rangle$ and the same M (or the same $\langle m_\beta \rangle$) exist and cannot be distinguished.

On the other hand, obviously, if one can determine that $\langle m_{\beta\beta} \rangle \geq 0.1$ eV we would conclude that the mass pattern is degenerate. And in the so far hypothetical case that one could show that $\langle m_{\beta\beta} \rangle \leq 0.01$ - 0.02 eV but nonvanishing nevertheless the normal hierarchy would be established[a].

It is worthwhile noting that if the inverted mass ordering is realized in nature, (and neutrinos are Majorana particles) the quantity $\langle m_{\beta\beta} \rangle$ is constrained from below by ~ 0.01 eV. This value is within reach of the next generation of experiments. Also, in principle, in the case of the normal hierarchy while all neutrinos could be massive Majorana particles it is still possible that $\langle m_{\beta\beta} \rangle = 0$. Such a situation, however, requires "fine tuning" or reflects a symmetry of some kind.

Let us remark that the $0\nu\beta\beta$ decay is not the only LNV process for which important experimental constraints exist. Examples of the other

[a] In that case also the $\langle m_\beta \rangle$ in the right panel would not represent the quatity directly related to the ordinary β decay. There are no realistic ideas, however, how to reach the corresponding sensitivity in ordinary β decay at this time.

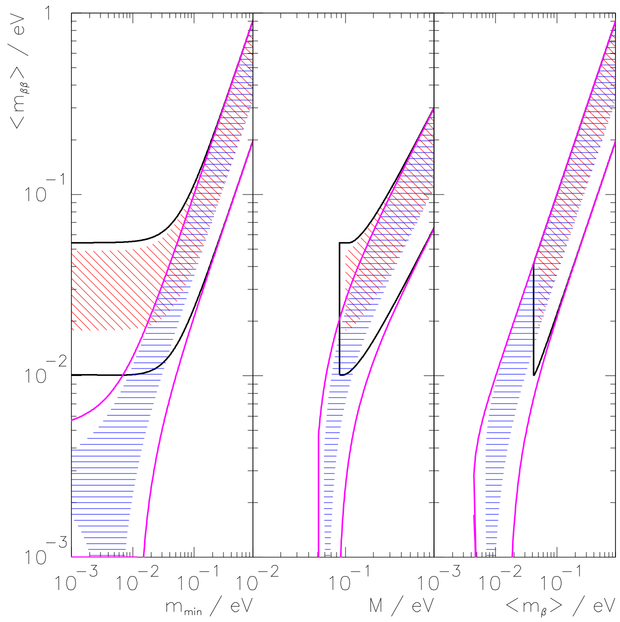

Fig. 10.5. The left panel shows the dependence of $\langle m_{\beta\beta}\rangle$ on the mass of the lightest neutrino m_{min}, the middle one shows the relation between $\langle m_{\beta\beta}\rangle$ and the sum of neutrino masses $M = \Sigma m_i$ determined or constrained by the "observational cosmology", and the right one depicts the relation between $\langle m_{\beta\beta}\rangle$ and the effective mass $\langle m_\beta\rangle$ determined or constrained by the ordinary β decay. In all panels the width of the hatched area is due to the unknown Majorana phases and therefore irreducible. The solid lines indicate the allowed regions by taking into account the current uncertainties in the oscillation parameters; they will shrink as the accuracy improves. The two sets of curves correspond to the normal and inverted hierarchies, they merge above about $\langle m_{\beta\beta}\rangle \geq 0.1$ eV, where the degenerate mass pattern begins.

analogous processes are

$$\begin{aligned}
&\mu^- + (Z,A) \rightarrow e^+ + (Z-2,A);\ \text{exp. branching ratio} \leq 10^{-12}\ , \\
&K^+ \rightarrow \mu^+\mu^+\pi^-;\ \text{exp. branching ratio} \leq 3\times 10^{-9}\ , \\
&\bar{\nu}_e \text{ emission from the Sun};\ \text{exp. branching ratio} \leq 10^{-4}\ . \qquad (10.4)
\end{aligned}$$

However, detailed analysis suggests that the study of the $0\nu\beta\beta$ decay is by far the most sensitive test of LNV. In simple terms, this is caused by the amount of tries one can make. A 100 kg $0\nu\beta\beta$ decay source contains $\sim 10^{27}$ nuclei. This can be contrasted with the possibilities of first producing muons or kaons, and then searching for the unusual decay channels. The Fermilab accelerators, for example, produce "a few" $\times 10^{20}$ protons on target per year in their beams and thus correspondingly smaller numbers of muons or kaons.

10.2. Mechanism of the $0\nu\beta\beta$ decay

It has been recognized long time ago that the relation between the $0\nu\beta\beta$ decay rate and the effective Majorana mass $\langle m_{\beta\beta}\rangle$ is to some extent problematic. The assumption leading to the eq.(**??**) is rather conservative, namely that there is an exchange of a virtual light, but massive, Majorana neutrino between the two nucleons undergoing the transition, and that these neutrinos interact by the standard left-handed weak currents. However, that is not the only possible mechanism. LNV interactions involving so far unobserved heavy ($\sim$ TeV) particles can lead to a comparable $0\nu\beta\beta$ decay rate. Thus, in the absence of additional information about the mechanism responsible for the $0\nu\beta\beta$ decay, one could not unambiguously infer $\langle m_{\beta\beta}\rangle$ from the $0\nu\beta\beta$ decay rate.

In general $0\nu\beta\beta$ decay can be generated by (i) light massive Majorana neutrino exchange or (ii) heavy particle exchange (see, e.g. Refs.[?,?]), resulting from LNV dynamics at some scale Λ above the electroweak one. The relative size of heavy (A_H) versus light particle (A_L) exchange contributions to the decay amplitude can be crudely estimated as follows:[?]

$$A_L \sim G_F^2 \frac{\langle m_{\beta\beta}\rangle}{\langle k^2\rangle},\ A_H \sim G_F^2 \frac{M_W^4}{\Lambda^5},\ \frac{A_H}{A_L} \sim \frac{M_W^4 \langle k^2\rangle}{\Lambda^5 \langle m_{\beta\beta}\rangle}\ , \tag{10.5}$$

where $\langle m_{\beta\beta}\rangle$ is the effective neutrino Majorana mass, $\langle k^2\rangle \sim (50\ \text{MeV})^2$ is the typical light neutrino virtuality, and Λ is the heavy scale relevant to the LNV dynamics. Therefore, $A_H/A_L \sim O(1)$ for $\langle m_{\beta\beta}\rangle \sim 0.1 - 0.5$ eV and $\Lambda \sim 1$ TeV, and thus the LNV dynamics at the TeV scale leads to similar $0\nu\beta\beta$ decay rate as the exchange of light Majorana neutrinos with the effective mass $\langle m_{\beta\beta}\rangle \sim 0.1 - 0.5$ eV.

Obviously, the lifetime measurement by itself does not provide the means for determining the underlying mechanism. The spin-flip and non-flip exchange can be, in principle, distinguished by the measurement of the single-electron spectra or polarization (see e.g.,[?]). However, in most cases the mechanism of light Majorana neutrino exchange, and of heavy particle exchange cannot be separated by the observation of the emitted electrons. Thus one must look for other phenomenological consequences of the different mechanisms other than observables directly associated with $0\nu\beta\beta$. Here I discuss the suggestion**?** that under natural assumptions the presence of low scale LNV interactions also affects muon lepton flavor violating (LFV) processes, and in particular enhances the $\mu \to e$ conversion compared to the $\mu \to e\gamma$ decay.

The discussion is concerned mainly with the branching ratios $B_{\mu\to e\gamma} = \Gamma(\mu \to e\gamma)/\Gamma_\mu^{(0)}$ and $B_{\mu\to e} = \Gamma_{\rm conv}/\Gamma_{\rm capt}$, where $\mu \to e\gamma$ is normalized to the standard muon decay rate $\Gamma_\mu^{(0)} = (G_F^2 m_\mu^5)/(192\pi^3)$, while $\mu \to e$ conversion is normalized to the corresponding capture rate $\Gamma_{\rm capt}$. The main diagnostic tool in the analysis is the ratio

$$\mathcal{R} = B_{\mu\to e}/B_{\mu\to e\gamma} \ , \tag{10.6}$$

and the relevance of our observation relies on the potential for LFV discovery in the forthcoming experiments MEG**?** ($\mu \to e\gamma$) and MECO**?** ($\mu \to e$ conversion)[b] that plan to improve the current limits by several orders of magnitude.

It is useful to formulate the problem in terms of effective low energy interactions obtained after integrating out the heavy degrees of freedom that induce LNV and LFV dynamics. If the scales for both LNV and LFV are well above the weak scale, then one would not expect to observe any signal in the forthcoming LFV experiments, nor would the effects of heavy particle exchange enter $0\nu\beta\beta$ at an appreciable level. In this case, the only origin of a signal in $0\nu\beta\beta$ at the level of prospective experimental sensitivity would be the exchange of a light Majorana neutrino, leading to eq.(**??**), and allowing one to extract $\langle m_{\beta\beta}\rangle$ from the decay rate.

In general, however, the two scales may be distinct, as in SUSY-GUT**?** or SUSY see-saw**?** models. In these scenarios, both the Majorana neutrino mass as well as LFV effects are generated at the GUT scale. The effects of heavy Majorana neutrino exchange in $0\nu\beta\beta$ are, thus, highly suppressed. In contrast, the effects of GUT-scale LFV are transmitted to the TeV-scale by a soft SUSY-breaking sector without mass suppression via renormalization group running of the high-scale LFV couplings. Consequently, such scenarios could lead to observable effects in the upcoming LFV experiments but with an $\mathcal{O}(\alpha)$ suppression of the branching ratio $B_{\mu\to e}$ relative to $B_{\mu\to e\gamma}$ due to the exchange of a virtual photon in the conversion process rather than the emission of a real one, thus $\mathcal{R} \sim 10^{-(2-3)}$ in this case.

[b] Even though MECO experiment was recently cancelled, proposals for experiments with similar sensitivity exist elsewhere.

The case where the scales of LNV and LFV are both relatively low ($\sim$ TeV) is more subtle. This is the scenario which might lead to observable signals in LFV searches and at the same time generate ambiguities in interpreting a positive signal in $0\nu\beta\beta$. Therefore, this is the case where one needs to develop some discriminating criteria.

Denoting the new physics scale by Λ, one has a LNV effective lagrangian of the form

$$\mathcal{L}_{0\nu\beta\beta} = \sum_i \frac{\tilde{c}_i}{\Lambda^5} \tilde{O}_i \qquad \tilde{O}_i = \bar{q}\Gamma_1 q \;\; \bar{q}\Gamma_2 q \, \bar{e}\Gamma_3 e^c \ , \tag{10.7}$$

where we have suppressed the flavor and Dirac structures (a complete list of the dimension nine operators $\tilde{O}_i$ can be found in Ref.[?]).

For the LFV interactions, one has

$$\mathcal{L}_{\rm LFV} = \sum_i \frac{c_i}{\Lambda^2} O_i \ , \tag{10.8}$$

and a complete operator basis can be found in Refs.[?,?] The LFV operators relevant to our analysis are of the following type (along with their analogues with $L \leftrightarrow R$):

$$\begin{aligned} O_{\sigma L} &= \frac{e}{(4\pi)^2} \overline{\ell_{iL}} \, \sigma_{\mu\nu} i \not{D} \, \ell_{jL} \ F^{\mu\nu} + \text{h.c.} \\ O_{\ell L} &= \overline{\ell_{iL}} \, \ell^c_{jL} \ \overline{\ell^c_{kL}} \, \ell_{mL} \\ O_{\ell q} &= \overline{\ell_i} \Gamma_\ell \ell_j \ \bar{q} \Gamma_q q \ . \end{aligned} \tag{10.9}$$

Operators of the type O_σ are typically generated at one-loop level, hence our choice to explicitly display the loop factor $1/(4\pi)^2$. On the other hand, in a large class of models, operators of the type O_ℓ or $O_{\ell q}$ are generated by tree level exchange of heavy degrees of freedom. With the above choices, all non-zero c_i and $\tilde{c}_i$ are nominally of the same size, typically the product of two Yukawa-like couplings or gauge couplings (times flavor mixing matrices).

With the notation established above, the ratio $\mathcal{R}$ of the branching ratios $\mu \to e$ to $\mu \to e{+}\gamma$ can be written schematically as follows (neglecting flavor indices in the effective couplings and the term with $L \leftrightarrow R$):

$$\begin{aligned} \mathcal{R} = \frac{\Phi}{48\pi^2} \Big| \lambda_1 \, e^2 c_{\sigma L} + e^2 \left(\lambda_2 c_{\ell L} + \lambda_3 c_{\ell q}\right) \log \frac{\Lambda^2}{m_\mu^2} \\ + \lambda_4 (4\pi)^2 c_{\ell q} \ + \ldots \Big|^2 \Big/ \left[e^2 \left(|c_{\sigma L}|^2 + |c_{\sigma R}|^2 \right) \right] \ . \end{aligned} \tag{10.10}$$

In the above formula $\lambda_{1,2,3,4}$ are numerical factors of $O(1)$, while the overall factor $\frac{\Phi}{48\pi^2}$ arises from phase space and overlap integrals of electron and muon wavefunctions in the nuclear field. For light nuclei $\Phi = (ZF_p^2)/(g_V^2 + 3g_A^2) \sim O(1)$ ($g_{V,A}$ are the vector and axial nucleon form factors at zero momentum transfer, while F_p is the nuclear form factor at $q^2 = -m_\mu^2$?). The dots indicate subleading terms, not relevant for our discussion, such as loop-induced contributions to c_ℓ and $c_{\ell q}$ that are analytic in external masses and momenta. In contrast the logarithmically-enhanced loop contribution given by the second term in the numerator of $\mathcal{R}$ plays an essential role. This term arises whenever the operators $O_{\ell L,R}$ and/or $O_{\ell q}$ appear at tree-level in the effective theory and generate one-loop renormalization of $O_{\ell q}$? (see Fig. **??**).

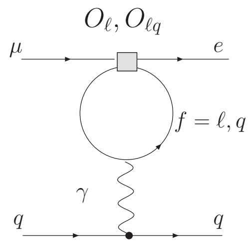

Fig. 10.6. Loop contributions to $\mu \to e$ conversion through insertion of operators O_ℓ or $O_{\ell q}$, generating the large logarithm.

The ingredients in eq. (**??**) lead to several observations: (i) In absence of tree-level $c_{\ell L}$ and $c_{\ell q}$, one obtains $\mathcal{R} \sim (\Phi\,\lambda_1^2\,\alpha)/(12\pi) \sim 10^{-3} - 10^{-2}$, due to gauge coupling and phase space suppression. (ii) When present, the logarithmically enhanced contributions compensate for the gauge coupling and phase space suppression, leading to $\mathcal{R} \sim O(1)$. (iii) If present, the tree-level coupling $c_{\ell q}$ dominates the $\mu \to e$ rate leading to $\mathcal{R} \gg 1$.

Thus, we can formulate our main conclusions regarding the discriminating power of the ratio $\mathcal{R}$:

(1) Observation of both the LFV muon processes $\mu \to e$ and $\mu \to e\gamma$ with relative ratio $\mathcal{R} \sim 10^{-2}$ implies, under generic conditions, that $\Gamma_{0\nu\beta\beta} \sim \langle m_{\beta\beta}\rangle^2$. Hence the relation of the $0\nu\beta\beta$ lifetime to the absolute neutrino mass scale is straightforward.
(2) On the other hand, observation of LFV muon processes with relative ratio $\mathcal{R} \gg 10^{-2}$ could signal non-trivial LNV dynamics at the TeV scale, whose effect on $0\nu\beta\beta$ has to be analyzed on a case by case basis.

Therefore, in this scenario no definite conclusion can be drawn based on LFV rates.

(3) Non-observation of LFV in muon processes in forthcoming experiments would imply either that the scale of non-trivial LFV and LNV is above a few TeV, and thus $\Gamma_{0\nu\beta\beta} \sim \langle m_{\beta\beta}\rangle^2$, or that any TeV-scale LNV is approximately flavor diagonal.

The above statements are illustrated using two explicit cases:[?] the minimal supersymmetric standard model (MSSM) with R-parity violation (RPV-SUSY) and the Left-Right Symmetric Model (LRSM).

RPV SUSY — If one does not impose R-parity conservation [$R = (-1)^{3(B-L)+2s}$], the MSSM superpotential includes, in addition to the standard Yukawa terms, lepton and baryon number violating interactions, compactly written as (see e.g.,[?])

$$\begin{aligned} W_{RPV} = \lambda_{ijk} L_i L_j E^c_k + \lambda'_{ijk} L_i Q_j D^c_k + \lambda''_{ijk} U^c_i D^c_j D^c_k \\ + \mu'_i L_i H_u \ , \end{aligned} \tag{10.11}$$

where L and Q represent lepton and quark doublet superfields, while E^c, U^c, D^c are lepton and quark singlet superfields. The simultaneous presence of λ' and λ'' couplings would lead to an unacceptably large proton decay rate (for SUSY mass scale $\Lambda_{SUSY} \sim$ TeV), so we focus on the case of $\lambda'' = 0$ and set $\mu' = 0$ without loss of generality. In such case, lepton number is violated by the remaining terms in W_{RPV}, leading to short distance contributions to $0\nu\beta\beta$ [e.g., Fig.**??**(a)], with typical coefficients [cf. eq. (**??**)]

$$\frac{\tilde{c}_i}{\Lambda^5} \sim \frac{\pi\alpha_s}{m_{\tilde{g}}} \frac{\lambda'^2_{111}}{m^4_{\tilde{f}}} \ ; \ \frac{\pi\alpha_2}{m_\chi} \frac{\lambda'^2_{111}}{m^4_{\tilde{f}}} \ , \tag{10.12}$$

where α_s, α_2 represent the strong and weak gauge coupling constants, respectively. The RPV interactions also lead to lepton number conserving but lepton flavor violating operators [e.g. Fig. **??**(b)], with coefficients [cf. eq. (**??**)]

$$\begin{aligned} \frac{c_\ell}{\Lambda^2} &\sim \frac{\lambda_{i11}\lambda^*_{i21}}{m^2_{\tilde{\nu}_i}}, \frac{\lambda^*_{i11}\lambda_{i12}}{m^2_{\tilde{\nu}_i}} \ , \\ \frac{c_{\ell q}}{\Lambda^2} &\sim \frac{\lambda'^*_{11i}\lambda'_{21i}}{m^2_{\tilde{d}_i}}, \frac{\lambda'^*_{1i1}\lambda'_{2i1}}{m^2_{\tilde{u}_i}} \ , \\ \frac{c_\sigma}{\Lambda^2} &\sim \frac{\lambda\lambda^*}{m^2_{\tilde{\ell}}}, \frac{\lambda'\lambda'^*}{m^2_{\tilde{q}}} \ , \end{aligned} \tag{10.13}$$

where the flavor combinations contributing to c_σ can be found in Ref.[?] Hence, for generic flavor structure of the couplings λ and λ' the underlying LNV dynamics generate both short distance contributions to $0\nu\beta\beta$ and LFV contributions that lead to $\mathcal{R} \gg 10^{-2}$.

Existing limits on rare processes strongly constrain combinations of RPV couplings, assuming Λ_{SUSY} is between a few hundred GeV and $\sim$ 1 TeV. Non-observation of LFV at future experiments MEG and MECO could be attributed either to a larger Λ_{SUSY} (> few TeV) or to suppression of couplings that involve mixing among first and second generations. In the former scenario, the short distance contribution to $0\nu\beta\beta$ does not compete with the long distance one [see eq. (**??**)], so that $\Gamma_{0\nu\beta\beta} \sim \langle m_{\beta\beta}\rangle^2$. On the other hand, there is an exception to this "diagnostic tool". If the λ and λ' matrices are nearly flavor diagonal, the exchange of superpartners may still make non-negligible contributions to $0\nu\beta\beta$ without enhancing the ratio $\mathcal{R}$.

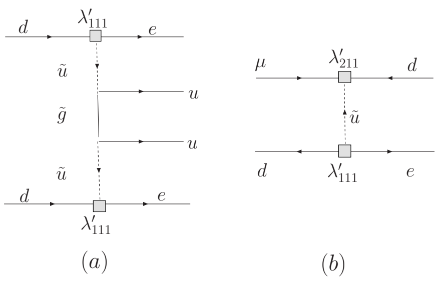

Fig. 10.7. Gluino exchange contribution to $0\nu\beta\beta$ (a), and typical tree-level contribution to $O_{\ell q}$ (b) in RPV SUSY.

LRSM — The LRSM provides a natural scenario for introducing non-sterile, right-handed neutrinos and Majorana masses.[?] The corresponding electroweak gauge group $SU(2)_L \times SU(2)_R \times U(1)_{B-L}$, breaks down to $SU(2)_L \times U(1)_Y$ at the scale $\Lambda \geq \mathcal{O}(\text{TeV})$. The symmetry breaking is implemented through an extended Higgs sector, containing a bi-doublet Φ and two triplets $\Delta_{L,R}$, whose leptonic couplings generate both Majorana neutrino masses and LFV involving charged leptons:

$$\begin{aligned}\mathcal{L}_Y^{\text{lept}} = &- \overline{L_L}^{\,i} \left(y_D^{ij}\, \Phi \ + \ \tilde{y}_D^{ij}\, \tilde{\Phi} \right) L_R^j \\ &- \overline{(L_L)^c}^{\,i}\, y_M^{ij}\, \tilde{\Delta}_L\, L_L^j \ - \ \overline{(L_R)^c}^{\,i}\, y_M^{ij}\, \tilde{\Delta}_R\, L_R^j \ .\end{aligned} \tag{10.14}$$

Here $\tilde{\Phi} = \sigma_2 \Phi^* \sigma_2$, $\tilde{\Delta}_{L,R} = i\sigma_2 \Delta_{L,R}$, and leptons belong to two isospin doublets $L^i_{L,R} = (\nu^i_{L,R}, \ell^i_{L,R})$. The gauge symmetry is broken through the VEVs $\langle \Delta^0_R \rangle = v_R$, $\langle \Delta^0_L \rangle = 0$, $\langle \Phi \rangle = \mathrm{diag}(\kappa_1, \kappa_2)$. After diagonalization of the lepton mass matrices, LFV arises from both non-diagonal gauge interactions and the Higgs Yukawa couplings. In particular, the $\Delta_{L,R}$-lepton interactions are not suppressed by lepton masses and have the structure $\mathcal{L} \sim \Delta^{++}_{L,R}\, \overline{\ell^c_i}\, h_{ij}\, (1 \pm \gamma_5) \ell_j + \text{h.c.}$. The couplings h_{ij} are in general non-diagonal and related to the heavy neutrino mixing matrix.[?]

Short distance contributions to $0\nu\beta\beta$ arise from the exchange of both heavy νs and $\Delta_{L,R}$ (Fig.**??**a), with

$$\frac{\tilde{c}_i}{\Lambda^5} \sim \frac{g_2^4}{M^4_{W_R}} \frac{1}{M_{\nu_R}} \; ; \; \frac{g_2^3}{M^3_{W_R}} \frac{h_{ee}}{M^2_{\Delta}} \; , \tag{10.15}$$

where g_2 is the weak gauge coupling. LFV operators are also generated through non-diagonal gauge and Higgs vertices, with[?] (Fig.**??**b)

$$\frac{c_\ell}{\Lambda^2} \sim \frac{h_{\mu i} h^*_{ie}}{m^2_\Delta} \qquad \frac{c_\sigma}{\Lambda^2} \sim \frac{(h^\dagger h)_{e\mu}}{M^2_{W_R}} \qquad i = e, \mu, \tau \; . \tag{10.16}$$

Note that the Yukawa interactions needed for the Majorana neutrino mass necessarily imply the presence of LNV and LFV couplings h_{ij} and the corresponding LFV operator coefficients c_ℓ, leading to $\mathcal{R} \sim O(1)$. Again, non-observation of LFV in the next generation of experiments would typically push Λ into the multi-TeV range, thus implying a negligible short distance contribution to $0\nu\beta\beta$. As with RPV-SUSY, this conclusion can be evaded by assuming a specific flavor structure, namely y_M approximately diagonal or a nearly degenerate heavy neutrino spectrum.

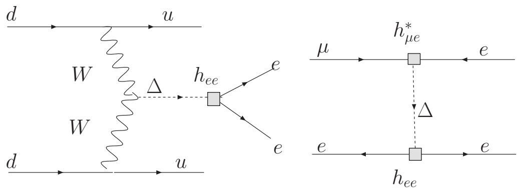

(a) (b)

Fig. 10.8. Typical doubly charged Higgs contribution to $0\nu\beta\beta$ (a) and to O_ℓ (b) in the LRSM.

In both of these phenomenologically viable models that incorporate LNV and LFV at low scale ($\sim$ TeV), one finds $\mathcal{R} \gg 10^{-2}$.[?,?,?] It is likely that the basic mechanism at work in these illustrative cases is generic: low scale LNV interactions ($\Delta L = \pm 1$ and/or $\Delta L = \pm 2$), which in general contribute to $0\nu\beta\beta$, also generate sizable contributions to $\mu \to e$ conversion, thus enhancing this process over $\mu \to e\gamma$.

In conclusion, the above considerations suggest that the ratio $\mathcal{R} = B_{\mu\to e}/B_{\mu\to e\gamma}$ of muon LFV processes will provide important insight about the mechanism of neutrinoless double beta decay and the use of this process to determine the absolute scale of neutrino mass. Assuming observation of LFV processes in forthcoming experiments, if $\mathcal{R} \sim 10^{-2}$ the mechanism of $0\nu\beta\beta$ is light Majorana neutrino exchange; if $\mathcal{R} \gg 10^{-2}$, there might be TeV scale LNV dynamics, and no definite conclusion on the mechanism of $0\nu\beta\beta$ can be drawn based only on LFV processes.

10.3. Overview of the experimental status of search for $\beta\beta$ decay

The field has a venerable history. The rate of the $2\nu\beta\beta$ decay was first estimated by Maria Goeppert-Mayer already in 1937 in her thesis work suggested by E. Wigner, basically correctly. Yet, first experimental observation in a laboratory experiment was achieved only in 1987, fifty years later. Why it took so long? As pointed out above, the typical half-life of the $2\nu\beta\beta$ decay is $\sim 10^{20}$ years. Yet, its "signature" is very similar to natural radioactivity, present to some extent everywhere, and governed by the half-life of $\sim 10^{10}$ years. So, background suppression is the main problem to overcome when one wants to study either of the $\beta\beta$ decay modes.

During the last two decades the $2\nu\beta\beta$ decay has been observed in "live" laboratory experiments in many nuclei, often by different groups and using different methods. That shows not only the ingenuity of the experimentalists who were able to overcome the background nemesis, but makes it possible at the same time to extract the corresponding 2ν nuclear matrix element from the measured decay rate. In the 2ν mode the half-life is given by

$$1/T_{1/2} = G^{2\nu}(Q,Z)|M^{2\nu}|^2 \ , \tag{10.17}$$

where $G^{2\nu}(Q,Z)$ is an easily and accurately calculable phase space factor.

The resulting nuclear matrix elements $M^{2\nu}$, which have the dimension energy^{-1}, are plotted in Fig.**??**. Note the pronounced shell dependence; the matrix element for ^{100}Mo is almost ten times larger than the one for ^{130}Te. Evaluation of these matrix elements, to be discussed below, is an important test for the nuclear theory models that aim at the determination of the analogous but different quantities for the 0ν neutrinoless mode.

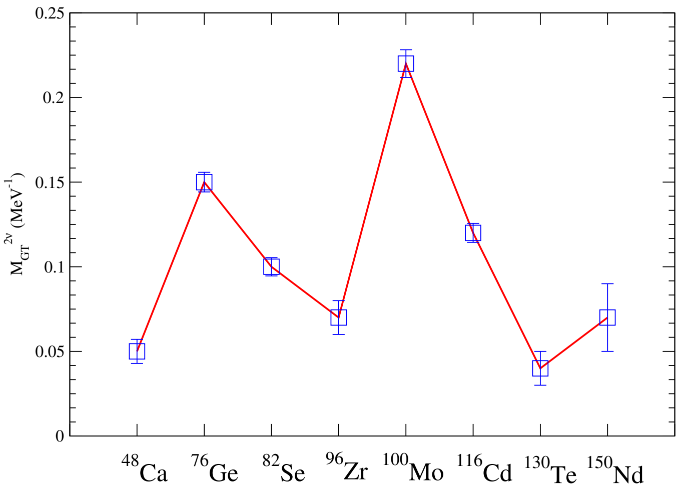

Fig. 10.9. Nuclear matrix elements for the $2\nu\beta\beta$ decay extracted from the measured half-lives.

The challenge of detecting the $0\nu\beta\beta$ decay is, at first blush, easier. Unlike the continuous $2\nu\beta\beta$ decay spectrum with a broad maximum at rather low energy where the background suppression is harder, the $0\nu\beta\beta$ decay spectrum is sharply peaked at the known Q value (see Fig.**??**), at energies that are not immune to the background, but a bit less difficult to manage. However, as also indicated in Fig.**??**, to obtain interesting results at the present time means to reach sensitivity to the 0ν half-lives that are $\sim 10^6$ times longer than the 2ν decay half-life of the same nucleus. So the requirements of background suppression are correspondingly even more severe.

The historical lessons are illustrated in Fig.**??** where the past limits on the $0\nu\beta\beta$ decay half-lives of various candidate nuclei are translated using the eq.(**??**) into the limits on the effective mass $\langle m_{\beta\beta}\rangle$. When plotted in the semi-log plot this figure represents the "Moore's law" of double beta decay, and indicates that, provided that the past trend will continue, the mass scale corresponding to Δm^2_{atm} will be reached in about 10 years.

This is also the time scale of significant experiments these days. Indeed, as discussed further, preparations are on the way to reach this sensitivity goal. Note that the figure was made using some assumed values of the corresponding nuclear matrix elements, without including their uncertainty. For such illustrative purposes they are, naturally, irrelevant.

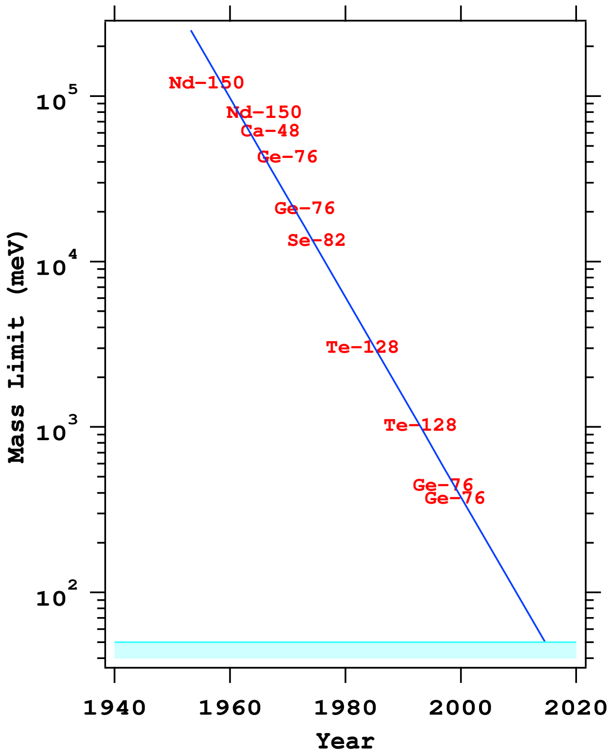

Fig. 10.10. The limit of the effective mass $\langle m_{\beta\beta} \rangle$ extracted from the experimental lower limits on the $0\nu\beta\beta$ decay half-life versus the corresponding year. The gray band near bottom indicates the $\sqrt{\Delta m^2_{atm}}$ value. Figure originally made by S. Elliott.

The past search for the neutrinoless double beta decay, illustrated in Fig.**??**, was driven by the then current technology and the resources of the individual experiments. The goal has been simply to reach sensitivity to longer and longer half-lives. The situation is different, however, now. The experimentalists at the present time can and do use the knowledge summarized in Fig.**??** to gauge the aim of their proposals. Based on that figure, the range of the mass parameter $\langle m_{\beta\beta} \rangle$ can be divided into three regions of interest.

- The degenerate mass region where all $m_i \gg \sqrt{\Delta m^2_{atm}}$. In that region $\langle m_{\beta\beta} \rangle \geq 0.1$ eV, corresponding crudely to the 0ν half-lives of 10^{26-27} years. To explore it (in a realistic time frame), ~ 100 kg of the decaying nucleus is needed. Several experiments aiming at such sensitivity are being built and should run and give results within the next 3-5 years. Moreover, this mass region (or a substantial part of it) will be explored, in a similar time frame, by the study of ordinary β decay (in particular of tritium) and by the observational cosmology. These techniques are independent on the Majorana nature of neutrinos. It is easy, but perhaps premature, to envision various scenarios depending on the possible outcome of these measurements.
- The so-called inverted hierarchy mass region where $20 < \langle m_{\beta\beta} \rangle < 100$ meV and the $0\nu\beta\beta$ half-lives are about 10^{27-28} years. (The name is to some extent a misnomer. In that interval one could encounter not only the inverted hierarchy but also a quasi-degenerate but normal neutrino mass ordering. Successful observation of the $0\nu\beta\beta$ decay will not be able to distinguish these possibilities, as I argued above. This is so not only due to the anticipated experimental accuracy, but more fundamentally due to the unknown Majorana phases.) To explore this mass region, $\sim$ ton size sources would be required. Proposals for the corresponding experiments exist, but none has been funded as yet, and presumably the real work will begin depending on the experience with the various ~ 100 kg size sources. Timeline for exploring this mass region is ~ 10 years.
- Normal mass hierarchy region where $\langle m_{\beta\beta} \rangle \leq$ 10-20 meV. To explore this mass region, ~ 100 ton sources would be required. There are no realistic proposals for experiments of this size at present.

Over the last two decades, the methodology for double beta decay experiments has improved considerably. Larger amounts of high-purity enriched parent isotopes, combined with careful selection of all surrounding materials and using deep-underground sites have lowered backgrounds and increased sensitivity. The most sensitive experiments to date use ^{76}Ge, ^{100}Mo, ^{116}Cd, ^{130}Te, and ^{136}Xe. For ^{76}Ge the lifetime limit reached impressive values exceeding 10^{25}years.[?,?] The experimental lifetime limits have been interpreted to yield effective neutrino mass limits typically a few eV and in ^{76}Ge as low as 0.3 - 1.0 eV (the spread reflects an estimate of the uncertainty in the nuclear matrix elements). The sum electron spectrum obtained in the Heidelberg-Moscow[?] experiment is shown in Fig.**??** over a broad energy range, and in Fig.**??** over a narrower range in the vicinity of the 0ν Q value of 2039 keV. Some residual natural radioactivity background lines are clearly visible in both figures, and no obvious peak at the 0ν expected position can be seen in Fig.**??**.

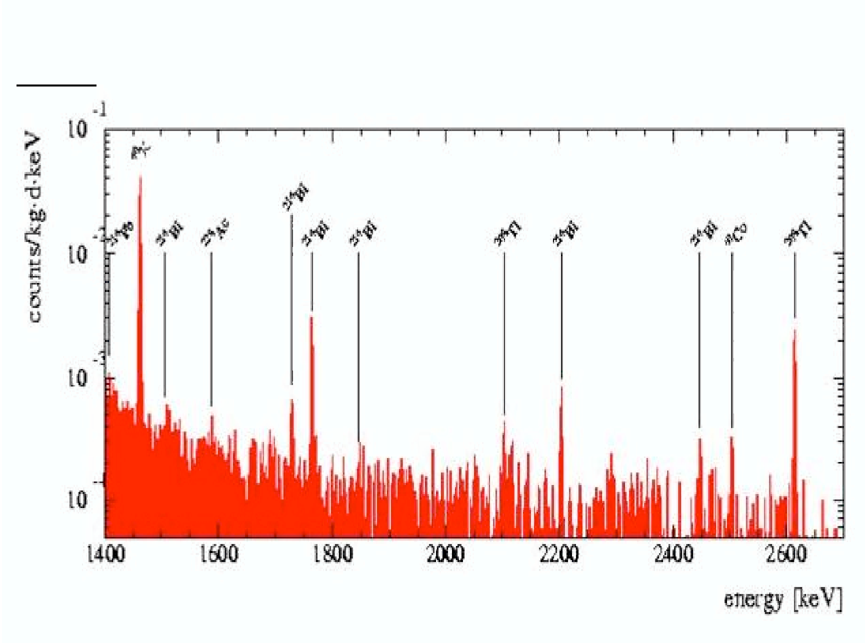

Fig. 10.11. The spectrum recorded in the Heidelberg-Moscow $\beta\beta$ decay experiment on ^{76}Ge. Identified γ lines are indicated.

Nevertheless, a subset of members of the Heidelberg-Moscow collaboration reanalyzed the data (and used additional information, e.g. the pulse-shape analysis and a different algorithm in the peak search) and claimed to observe a positive signal corresponding to the effective mass of $\langle m_{\beta\beta} \rangle = 0.39^{+0.17}_{-0.28}$ eV.[?] That report has been followed by a lively discussion. Clearly, such an extraordinary claim with its profound implications, requires extraordinary evidence. It is fair to say that a confirmation, both for the same ^{76}Ge parent nucleus, and better yet also in another nucleus

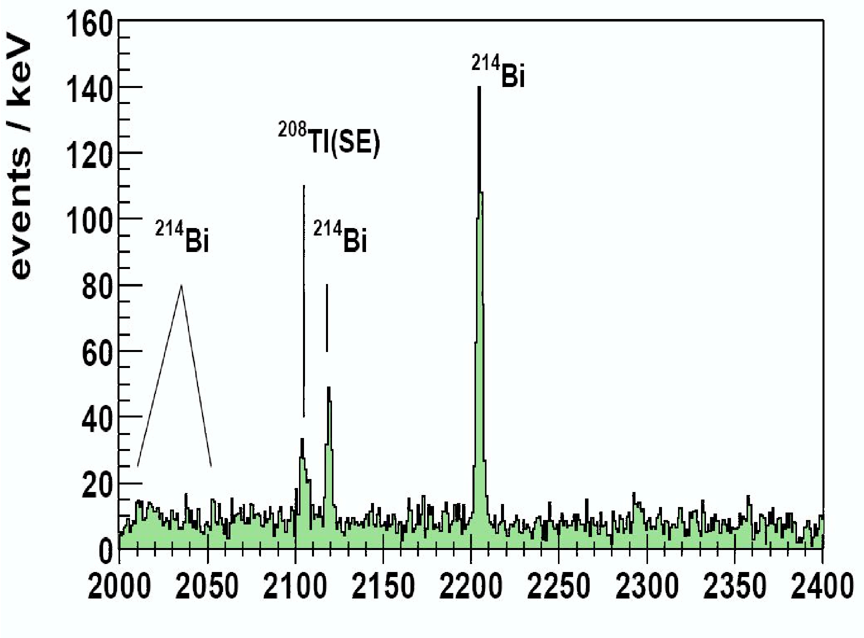

Fig. 10.12. Spectrum of the Heidelberg-Moscow experiment in the vicinity of the $0\nu\beta\beta$ decay value of 2039 keV.

with a different Q value, would be required for a consensus. In any case, if that claim is eventually confirmed, the degenerate mass scenario will be implicated, and eventual positive signal in the analysis of the tritium β decay and/or observational cosmology should be forthcoming. For the neutrinoless $\beta\beta$ decay the next generation of experiments, which use $\sim$ 100 kg of decaying isotopes will, among other things, test this recent claim.

It is beyond the scope of these lecture notes to describe in detail the forthcoming $0\nu\beta\beta$ decay experiments. Rather detailed discussion of them can be found e.g. in Ref.[?] Also, the corresponding chapter of the APS neutrino study[?] has various details. Nevertheless, let me briefly comment on the most advanced of the forthcoming $\sim$ 100 kg source experiments *CUORE, GERDA, EXO,* and *MAJORANA*. All of them are designed to explore all (or at least most) of the degenerate neutrino mass region $\langle m_{\beta\beta}\rangle \geq$ 0.1 eV. If their projected efficiencies and background projections are confirmed, all of them plan to consider scaling up the decaying mass to $\sim$ ton and extend their sensitivity to the "inverted hierarchy" region.

These experiments use different nuclei as a source, ^{76}Ge for *GERDA* and *MAJORANA*, ^{130}Te for *CUORE*, and ^{136}Xe for *EXO*. The requirement of radiopurity of the source material and surrounding auxiliary equipment is common to all of them, as is the placement of the experiment deep underground to shield against cosmic rays. The way the electrons are detected is, however, different. While the germanium detectors with their superb energy resolution have been used for the search of the $0\nu\beta\beta$ decay for a long time, the cryogenic detectors in *CUORE* use the temperature increase associated with an event in the very cold TeO_2 crystals, and in the *EXO* experiment a Time Projection Chamber (TPC) uses both scintillation and ionization to detect the events. The *EXO* experiment in its final form (still under development and very challenging) would use a positive identification of the final Ba^+ ion as an ultimate background rejection tool. These four experiments are in various stages of funding and staging. First results are expected in about 3 years, and substantial results within 3-5 years in all of them.

10.4. Nuclear matrix elements

It follows from eq.(**??**) that (i) values of the nuclear matrix elements $M^{0\nu}$ are needed in order to extract the effective neutrino mass from the measured $0\nu\beta\beta$ decay rate, and (ii) any uncertainty in $M^{0\nu}$ causes a corresponding and equally large uncertainty in the extracted $\langle m_{\beta\beta} \rangle$ value. Thus, the issue of an accurate evaluation of the nuclear matrix elements attracts considerable attention.

To see qualitatively where the problems are, let us consider the so-called closure approximation, i.e. a description in which the second order perturbation expression is approximated as

$$M^{0\nu} \equiv \langle \Psi_{final} | \hat{O}^{(0\nu)} | \Psi_{initial} \rangle \ . \tag{10.18}$$

Now, the challenge is to use an appropriate many-body nuclear model to describe accurately the wave functions of the ground states of the initial and final nuclei, $|\Psi_{initial}\rangle$ and $|\Psi_{final}\rangle$, as well as the appropriate form of the effective transition operator $\hat{O}^{(0\nu)}$ that describes the transformation of two neutrons into two protons correlated by the neutrino propagator, and consistent with the approximations inherent to the nuclear model used.

Common to all methods is the description of the nucleus as a system of nucleons bound in the mean field and interacting by an effective residual interaction. The used methods differ as to the number of nucleon orbits (or shells and subshells) included in the calculations and the complexity of the configurations of the nucleons in these orbits. The two basic approaches used so far for the evaluation of the nuclear matrix elements for both the 2ν and 0ν $\beta\beta$ decay modes are the Quasiparticle Random Phase Approximation (QRPA) and the nuclear shell model (NSM). They are in some sense complementary; QRPA uses a larger set of orbits, but truncates heavily the included configurations, while NSM can include only a rather small set of orbits but includes essentially all possible configurations. NSM also can be tested in a considerable detail by comparing to the nuclear spectroscopy data; in QRPA such comparisons are much more limited.

For the 2ν decay one can relate the various factors entering the calculations to other observables (β strength functions, cross sections of the charge-exchange reactions, etc.), accessible to the experiment. The consistency of the evaluation can be tested in that way. Of course, as pointed out above (see Fig.**??**) the nuclear matrix elements for this mode are known anyway. Both methods are capable of describing the 2ν matrix elements, at least qualitatively. These quantities, when expressed in natural units based on the sum rules, are very small. Hence their description depends on small components of the nuclear wave functions and is therefore challenging. In QRPA the agreement is achieved if the effective proton-neutron interaction coupling constant (usually called g_{pp}) is slightly (by $\sim$ 10 - 20 %) adjusted.

The theoretical description for the more interesting 0ν mode cannot use any known nuclear observables, since there are no observables directly related to the $M^{0\nu}$. It is therefore much less clear how to properly estimate the uncertainty associated with the calculated values of $M^{0\nu}$, and to judge their accuracy. Since the calculations using QRPA are much simpler, an overwhelming majority of the published calculations uses that method. There are suggestions to use the spread of these published values of $M^{0\nu}$ as a measure of uncertainty.[?] Following this, one would conclude that the uncertainty is quite large, a factor of three or as much as five. But that way of assigning the uncertainty is questionable. Using all or most of the published values of $M^{0\nu}$ means that one includes calculations of uneven quality. Some of them were devoted to the tests of various approximations, and concluded that they are not applicable. Some insist that other data, like the $M^{2\nu}$, are correctly reproduced, other do not pay any attention to such test. Also, different forms of the transition operator $\hat{O}^{0\nu}$ are used, in particular some works include approximately the effect of the short range nucleon-nucleon repulsion, while others neglect it.

In contrast, in Ref.[?] an assesment of uncertainties in the matrix elements $M^{0\nu}$ inherent in the QRPA was made, and it was concluded that with a consistent treatment the uncertainties are much less, perhaps only about 30% (see Fig.**??**). That calculation uses the known 2ν matrix elements in order to adjust the interaction constant mentioned above. There is a lively debate in the nuclear structure theory community, beyond the scope of these lectures, about this conclusion.

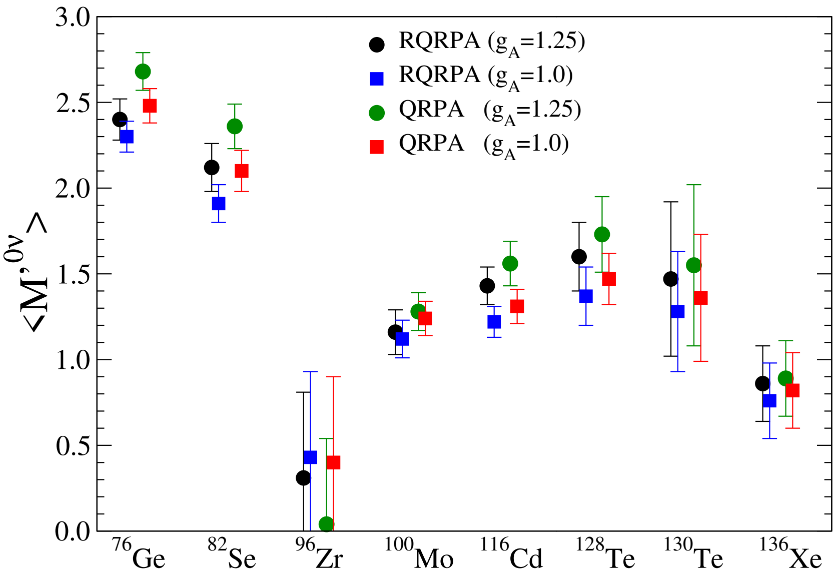

Fig. 10.13. Nuclear matrix elements and their variance for the indicated approximations (see Ref.[?]).

It is of interest also to compare the resulting matrix elements of Rodin et al.[?] based on QRPA and its generalizations, and those of the available most recent NSM evaluation.[?] Note that the operators used in NSM evaluation do not include the induced nucleon currents that in QRPA reduce the matrix element by about 30%. The QRPA[?] and NSM[?] $M^{0\nu}$ are compared in Table **??**. In the last column the NSM matrix elements are reduced by 30% to approximately account for the missing terms in the operator, and to make the comparison more meaningful. With this reduction, it seems that QRPA results are a bit larger in the lighter nuclei and a bit

Table 10.1. Comparison of the calculated nuclear matrix elements $M^{0\nu}$ using the QRPA method[?] and the NSM.[?] In the last column the NSM values are reduced, divided by 1.3, to account approximately for the effects of the induced nucleon currents.

Nucleus	QRPA	NSM	NSM/1.3
^{76}Ge	2.3-2.4	2.35	1.80
^{82}Se	1.9-2.1	2.26	1.74
^{96}Zr	0.3-0.4		
^{100}Mo	1.1-1.2		
^{116}Cd	1.2-1.4		
^{130}Te	1.3	2.13	1.64
^{136}Xe	0.6-1.0	1.77	1.36

smaller in the heavier ones than the NSM results, but basically within the 30% uncertainty estimate. Once the NSM calculations for the intermediate mass nuclei ^{96}Zr, ^{100}Mo and ^{116}Cd become available, one can make a more meaningful comparison of the two methods.

When comparing the results shown in Table **??** as well as the results of other calculations (e.g. Refs.[?,?]) with Fig. **??** it is important to notice a qualitative difference in the behaviour of the 2ν and 0ν matrix elements when going from one nucleus to another one. For 2ν the matrix elements change rapidly, but for the 0ν the variation is much more gentle (^{96}Zr is a notable exception, at least for QRPA). That feature, common to most calculations, if verified, would help tremendously in comparing the results or constraints from one nucleus to another one.

Once the nuclear matrix elements are fixed (by choosing your favorite set of results), they can be combined with the phase space factors (a complete list is available, e.g. in the monograph[?]) to obtain a half-life prediction for any value of the effective mass $\langle m_{\beta\beta} \rangle$. It turns out that for a fixed $\langle m_{\beta\beta} \rangle$ the half-lives of different candidate nuclei do not differ very much from each other (not more than by factors ~ 3 or so) and, for example, the boundary between the degenerate and inverted hierarchy mass regions corresponds to half-lives $\sim 10^{27}$years. Thus, the next generation of experiments, discussed above, should reach this region using several candidate nuclei, making the corresponding conclusions less nuclear model dependent.

10.5. Neutrino magnetic moment and the distinction between Dirac and Majorana neutrinos

Neutrino mass and magnetic moments are intimately related. In the orthodox Standard Model neutrinos have a vanishing mass and magnetic moments vanish as well. However, in the minimally extended SM containing gauge-singlet right-handed neutrinos the magnetic moment μ_ν is nonvanishing and proportional to the neutrino mass, but unobservably small,[?]

$$\mu_\nu = \frac{3eG_F}{\sqrt{2}8\pi^2} m_\nu = 3 \times 10^{-19} \mu_B \frac{m_\nu}{1 \text{ eV}} \ . \tag{10.19}$$

Here μ_B is the electron Bohr magneton, traditionally used as unit also for the neutrino magnetic moments. An experimental observation of a magnetic moment larger than that given in eq.(**??**) would be an uneqivocal indication of physics beyond the minimally extended Standard Model.

Laboratory searches for neutrino magnetic moments are typically based on the obsevation of the $\nu - e$ scattering. Nonvanishing μ_ν will be recognizable only if the corresponding electromagnetic scattering cross section is at least comparable to the well understood weak interaction cross section. The magnitude of μ_ν (diagonal in flavor or transitional) which can be probed in this way is then given by

$$\frac{|\mu_\nu|}{\mu_B} \equiv \frac{G_F m_e}{\sqrt{2}\pi\alpha} \sqrt{m_e T} \sim 10^{-10} \left(\frac{T}{m_e} \right)^{1/2} \ , \tag{10.20}$$

where T is the electron recoil kinetic energy. Considering realistic values of T, it would be difficult to reach sensitivities below $\sim 10^{-11} \mu_B$. Present limits are about an order of magnitude larger than that.

Limits on μ_ν can also be obtained from bounds on the unobserved energy loss in astrophysical objects. For sufficiently large μ_ν the rate of plasmon decay into the $\nu\bar{\nu}$ pairs would conflict with such bounds. Since plasmons can also decay weakly into the $\nu\bar{\nu}$ pairs , the sensitivity of this probe is again limited by the size of the weak rate, leading to

$$\frac{|\mu_\nu|}{\mu_B} \equiv \frac{G_F m_e}{\sqrt{2}\pi\alpha} \hbar\omega_P \ , \tag{10.21}$$

where ω_P is the plasmon frequency. Since usually $(\hbar\omega_P)^2 \ll m_e T$ that limit is stronger than that given in eq.(**??**). Current limits on μ_ν based on such considerations are $\sim 10^{-12} \mu_B$.

The interest in μ_ν and its relation to neutrino mass dates from $\sim$1990 when it was suggested that the chlorine data[?] on solar neutrinos show an anticorrelation between the neutrino flux and the solar activity characterized by the number of sunspots. A possible explanation was suggested in Ref.[?] where it was proposed that a magnetic moment $\mu_\nu \sim 10^{-(10-11)}\mu_B$ would cause a precession in solar magnetic field of the neutrinos emitted initially as left-handed ν_e into unobservable right-handed ones. Even though later analyses showed that the correlation with solar acivity does not exist, the possibility of a relatively large μ_ν accompanied by a small mass m_ν was widely discussed and various models accomplishing that were suggested.

If a magnetic moment is generated by physics beyond the Standard Model (SM) at an energy scale Λ, we can generically express its value as

$$\mu_\nu \sim \frac{eG}{\Lambda}, \tag{10.22}$$

where e is the electric charge and G contains a combination of coupling constants and loop factors. Removing the photon from the diagram gives a contribution to the neutrino mass of order

$$m_\nu \sim G\Lambda. \tag{10.23}$$

We thus arrive at the relationship

$$m_\nu \sim \frac{\Lambda^2}{2m_e}\frac{\mu_\nu}{\mu_B} \quad \sim \frac{\mu_\nu}{10^{-18}\mu_B}[\Lambda(\mathrm{TeV})]^2 \ \mathrm{eV}, \tag{10.24}$$

which implies that it is difficult to simultaneously reconcile a small neutrino mass and a large magnetic moment.

This naïve restriction given in eq.(**??**) can be overcome via a careful choice for the new physics, e.g., by requiring certain additional symmetries.[?,?,?,?,?,?] Note, however, that these symmetries are typically broken by Standard Model interactions. For Dirac neutrinos such symmetry (under which the left-handed neutrino and antineutrino ν and ν^c transform as a doublet) is violated by SM gauge interactions. For Majorana neutrinos analogous symmetries are not broken by SM gauge interactions, but are instead violated by SM Yukawa interactions, provided that the charged lepton masses are generated via the standard mechanism through Yukawa couplings to the SM Higgs boson. This suggests that the relation between μ_ν and m_ν is different for Dirac and Majorana neutrinos. This distinction can be, at least in principle, exploited experimentally, as shown below.

Earlier, I have quoted the Ref.[?] (see Fig.**??**) to stress that observation of the $0\nu\beta\beta$ decay would necessarily imply the existence of a novanishing neutrino Majorana mass. Analogous considerations can be applied in this case. By calculating neutrino magnetic moment contributions to m_ν generated by SM radiative corrections, one may obtain in this way general, "naturalness" upper limits on the size of neutrino magnetic moments by exploiting the experimental upper limits on the neutrino mass.

In the case of Dirac neutrinos, a magnetic moment term will generically induce a radiative correction to the neutrino mass of order[?]

$$m_\nu \sim \frac{\alpha}{16\pi} \frac{\Lambda^2}{m_e} \frac{\mu_\nu}{\mu_B} \quad \sim \frac{\mu_\nu}{3 \times 10^{-15} \mu_B} [\Lambda(\mathrm{TeV})]^2 \ \mathrm{eV}. \tag{10.25}$$

Taking $\Lambda \simeq 1$ TeV and $m_\nu \leq 0.3$ eV, we obtain the limit $\mu_\nu \leq 10^{-15} \mu_B$ (and a more stringent one for larger Λ), which is several orders of magnitude more constraining than current experimental upper limits on μ_ν.

The case of Majorana neutrinos is more subtle, due to the relative flavor symmetries of m_ν and μ_ν respectively. For Majorana neutrinos the transition magnetic moments $[\mu_\nu]_{\alpha\beta}$ (the only possible ones) are antisymmetric in the flavor indices $\{\alpha, \beta\}$, while the mass terms $[m_\nu]_{\alpha\beta}$ are symmetric. These different flavor symmetries play an important role in the limits, and are the origin of the difference between the magnetic moment constraints for Dirac and Majorana neutrinos.

It has been shown in Ref.[?] that the constraints on Majorana neutrinos are significantly weaker than those for Dirac neutrinos,[?] as the different flavor symmetries of m_ν and μ_ν lead to a mass term which is suppressed only by charged lepton masses. This conclusion was reached by considering one-loop mixing of the magnetic moment and mass operators generated by Standard Model interactions. The authors of Ref.[?] found that if a magnetic moment arises through a coupling of the neutrinos to the neutral component of the $SU(2)_L$ gauge boson, the constraints for $\mu_{\tau e}$ and $\mu_{\tau\mu}$ are comparable to present experiment limits, while the constraint on $\mu_{e\mu}$ is significantly weaker. Thus, the analysis of Ref.[?] lead to a bound for the transition magnetic moment of Majorana neutrinos that is less stringent than present experimental limits.

Even more generally it was shown in Ref.[?] that two-loop matching of mass and magnetic moment operators implies stronger constraints than those obtained in[?] if the scale of the new physics $\Lambda \geq 10$ TeV. Moreover, these constraints apply to a magnetic moment generated by either the hypercharge or $SU(2)_L$ gauge boson. In arriving at these conclusions, the most general set of operators that contribute at lowest order to the mass and magnetic moments of Majorana neutrinos was constructed, and model independent constraints which link the two were obtained. Thus the results of Ref.[?] imply completely model independent naturalness bound that – for $\Lambda \geq 100$ TeV – is stronger than present experimental limits (even for the weakest constrained element $\mu_{e\mu}$). On the other hand, for sufficiently low values of the scale Λ the known small values of the neutrino masses do not constrain the magnitude of the transition magnetic moment μ_ν for Majorana neutrinos more than the present experimental limits. Thus, if these conditions are fulfilled, the discovery of μ_ν might be forthcoming any day.

The above result means that an experimental discovery of a magnetic moment near the present limits would signify that (i) neutrinos are Majorana fermions and (ii) new lepton number violating physics responsible for the generation of μ_ν arises at a scale Λ which is well below the see-saw scale. This would have, among other things, implications for the mechanism of the neutrinoless double beta decay and lepton flavor violation as discussed above and in Ref.[?]

10.6. Summary

In these lectures I discussed the status of double beta decay, its relation to the charge conjugation symmetry of neutrinos and to the problem of the lepton number conservation in general. I have shown that if one makes the minimum assumption that the light neutrinos familiar from the oscillation experiments which are interacting by the left-handed weak current are Majorana particles, then the rate of the $0\nu\beta\beta$ decay can be related to the absolute scale of the neutrino mass in a straightforward way.

On the other hand, it is also possible that the $0\nu\beta\beta$ decay is mediated by the exchange of heavy particles. I explained that if the corresponding mass scale of such hypothetical particles is ~ 1 TeV, the corresponding 0ν decay rate could be comparable to the decay rate associated with the exchange of a light neutrino. I further argued that the study of the lepton flavor violation involving $\mu \to e$ conversion and $\mu \to e + \gamma$ decay may be used as a "diagnostic tool" that could help to decide which of the possible mechanisms of the 0ν decay is dominant.

Further, I have shown that the the range of the effective masses $\langle m_{\beta\beta} \rangle$ can be roughly divided into three regions of interest, each corresponding to a different neutrino mass pattern. The region of $\langle m_{\beta\beta} \rangle \geq 0.1$ eV corresponds to the degenerate mass pattern. Its exploration is well advanced, and one can rather confidently expect that it will be explored by several $\beta\beta$ decay experiments in the next 3-5 years. This region of neutrino masses (or most of it) is also accessible to studies using the ordinary β decay and/or the observational cosmology. Thus, if the nature is kind enough to choose this mass pattern, we will have a multiple ways of exploring it.

The region of $0.01 \leq \langle m_{\beta\beta} \rangle \leq 0.1$ eV is often called the "inverted mass hierarchy" region. In fact, both the inverted and the quasi-degenerate but normal mass orderings are possible in this case, and experimentally indistinguishable. Realistic plans to explore this region using the $0\nu\beta\beta$ decay exist, but correspond to a longer time scale of about 10 years. They require much larger, $\sim$ ton size $\beta\beta$ sources and correspondingly even more stringent background suppression.

Finally, the region $\langle m_{\beta\beta} \rangle \leq 0.01$ eV corresponds to the normal hierarchy only. There are no realistic proposals at present to explore this mass region experimentally.

Intimately related to the extraction of $\langle m_{\beta\beta} \rangle$ from the decay rates is the problem of nuclear matrix elements. At present, there is no consensus among the nuclear theorists about their correct values, and the corresponding uncertainty. I argued that the uncertainty is less than some suggest, and that the closeness of the Quasiparticle Random Phase Approximation (QRPA) and Shell Model (NSM) results are encouraging. But this is still a problem that requires further improvements.

In the last part I discussed the neutrino magnetic moments. I have shown that using the Standard Model radiative correction one can calculate the contribution of the magnetic moment to the neutrino mass. That contribution, naturally, should not exceed the experimental upper limit on the neutrino mass. Using this procedure one can show that the magnetic moment of Dirac neutrinos cannot exceed about $10^{-15}\mu_B$, which is several orders of magnitudes less than the current experimental limits on μ_ν. On the other hand, due to the different symmetries of the magnetic moment and mass matrices for Majorana neutrinos, the corresponding constraints are much less restrictive, and do not exceed the current limits. Thus, a discovery of μ_ν near the present experimental limit would indicate that neutrinos are Majorana particles, and the corresponding new physics scale is well below the GUT scale.

Acknowlegment

The original results reported here were obtained in the joint and enjoyable work with a number of collaborators, Nicole Bell, Vincenzo Cirigliano, Steve Elliott, Amand Faessler, Michail Gorchtein, Andriy Kurylov, Gary Prezeau, Michael Ramsey-Musolf, Vadim Rodin, Fedor Šimkovic and Mark

Wise. The work was supported in part under U.S. DOE contract DE-FG02-05ER41361.

References

1. T. Kajita and Y. Totsuka , *Rev. Mod. Phys.* **73**, 85-118 (2001); Y. Ashie et al., *Phys. Rev.* **D71**, 112005 (2005).
2. M. H. Ahn . *et al.*, *Phys. Lett. B* **511**, 178-184 (2001); M. H. Ahn *et al.* hep-ex/0606032.
3. MINOS collaboration, hep-ex/0607088
4. B. T. Cleveland *et al.*, *Astrophys. J.* **496**, 505 (1998).
5. Q. R. Ahmad *et al.*, *Phys. Rev. Lett.* **87**, 071301 (2001).
6. S. Fukuda *et al.*, *Phys. Rev. Lett.* **86**, 5651-5655, (2001); ibid **86**, 5656-5660 (2001).
7. W. Hampel *et al. Phys. Lett.* **B447**, 127 (1999).
8. J. N. Abdurashitov *et al. Phys. Rev.* **C60**, 055801 (1999).
9. K. Eguchi *et al. Phys. Rev. Lett.* **90**, 021802 (2003).
10. T. Araki *et al. Phys. Rev. Lett.* **94**, 081801 (2005).
11. M. Apollonio *et al.*, *Phys. Lett. B* **466**, 415-430 (1999).
12. F. Boehm *et al.*, *Phys. Rev.* **D64**, 112001 (2001).
13. A. Faessler and F. Šimkovic,F. Šimkovic, *J. Phys. G* **24**, 2139 (1998).
14. J. D. Vergados, *Phys. Rep.* **361**, 1 (2002).
15. S. R. Elliott and P. Vogel *Ann.Rev.Nucl.Part.Sci.* **52**, 115 (2002).
16. S. R. Elliott and J. Engel, *J. Phys. G* **30**, R183 (2004).
17. J. Schechter and J. Valle, *Phys.Rev.* **D25**, 2951 (1982).
18. R. N. Mohapatra, Phys. Rev. D**34**, 3457(1986); J. D. Vergados, Phys. Lett. **B184**, 55(1987); M. Hirsch, H. V. Klapdor-Kleingrothaus, and S. G. Kovalenko, Phys. Rev. D**53**, 1329(1996); M. Hirsch, H. V. Klapdor-Kleingrothaus, and O. Panella, Phys. Lett. **B374**, 7(1996); A. Fässler, S. Kovalenko, F. Šimkovic, and J. Schwieger, Phys. Rev. Lett. **78**, 183(1997); H. Päs, M. Hirsch, H. V. Klapdor-Kleingrothaus, and S. G. Kovalenko, Phys. Lett. **B498**, 35(2001). F. Šimkovic and A. Fässler, Progr. Part. Nucl. Phys. **48**, 201(2002).
19. G. Prezeau, M. Ramsey-Musolf and P. Vogel, Phys. Rev. D **68**, 034016 (2003).
20. R. N. Mohapatra, Nucl. Phys. Proc. Suppl. **77**, 376 (1999).
21. M. Doi, T. Kotani, and E. Takasugi, Prog. Theor. Phys. Suppl. **83**, 1(1985).
22. V. Cirigliano, A. Kurylov, M. J. Ramsey-Musolf and P. Vogel, *Phys.Rev.Lett*93, 231802 (2004).
23. G. Signorelli, "The Meg Experiment At Psi: Status And Prospects,"m J. Phys. G **29**, 2027 (2003); see also http://meg.web.psi.ch/docs/index.html.
24. J. L. Popp, NIM **A472**, 354 (2000); hep-ex/0101017.
25. R. Barbieri, L. J. Hall and A. Strumia, Nucl. Phys. B **445**, 219 (1995)
26. F. Borzumati and A. Masiero *Phys.Rev.Lett.***57**, 961 (1986).
27. M. Raidal and A. Santamaria, Phys. Lett. B **421**, 250 (1998).

28. R. Kitano, M. Koike and Y. Okada, Phys. Rev. D **66**, 096002 (2002).
29. H. K. Dreiner, in 'Perspectives on Supersymmetry', Ed. by G.L. Kane, World Scientific, 462-479.
30. A. de Gouvea, S. Lola and K. Tobe, Phys. Rev. D **63**, 035004 (2001).
31. R. N. Mohapatra and G. Senjanovic, Phys. Rev. Lett. **44**, 912 (1980).
32. V. Cirigliano, A. Kurylov, M. J. Ramsey-Musolf and P. Vogel, *Phys. Rev.* **D70**, 075007 (2004).
33. H. V. Klapdor-Kleingrothaus *et al. Eur.J.Phys.* **A12**, 147 (2001).
34. C. E. Aalseth *et al. Phys.Rev.* **D65**, 092007 (2002).
35. H. V. Klapdor-Kleingrothaus, A. Dietz, I. V. Krivosheina, and). Chvorets, *Phys. Lett.* **B586**, 198 (2004); *Nucl. Inst. Meth* **A522**, 371 (2004).
36. C. E. Aalseth *et al.*, hep-ph/0412300.
37. J. N. Bahcall, H. Murayama, and C. Pena-Garay, *Phys. Rev.***D70**, 033012 (2004).
38. V.A.Rodin, Amand Faessler, F. Šimkovic and Petr Vogel, *Phys. Rev.* **C68**, 044302(2003); *Nucl. Phys.* **A766**, 107 (2006).
39. A. Poves, talk at NDM06, http://events.lal.in2p3.fr/conferences/NDM06/.
40. O. Civitarese and J. Suhonen, *Nucl. Phys.* **A729**, 867 (2003).
41. Aunola M. and Suhonen J., *Nucl. Phys.* **A643**, 207 (1998).
42. F. Boehm and P. Vogel, *Physics of Massive Neutrinos*, 2nd ed., Cambridge University Press, Cambridge, UK. 1992.
43. W. J. Marciano and A. I. Sanda, *Phys. Lett.* **B67**, 303 (1977); B. W. Lee and R. E. Shrock, *Phys. Rev.* **D16**, 1444 (1977); K. Fujikawa and R. E. Shrock, *Phys. Rev. Lett.* **45**, 963 (1980).
44. M. B. Voloshin, M. I. Vysotskij and L. B. Okun, *Soviet J. of Nucl. Phys.* **44**, 440 (1986).
45. M. B. Voloshin, *Soviet J. of Nucl. Phys.* **48**, 512 (1988).
46. R. Barbieri and R. N. Mohapatra, *Phys. Lett.* **B218**, 225 (1989.
47. H. Georgi and L. Randall, *Phys. Lett.* **B244**, 196 (1990).
48. W. Grimus and H. Neufeld, *Nucl. Phys.* **B351**, 115 (1991).
49. K. S. Babu and R. N. Mohapatra, *Phys. Rev. Lett.* **64**, 1705 (1990).
50. S. M. Barr, E. M. Freie and A. Zee, *Phys. Rev. Lett.* **65**, 2626 (1990).
51. N. F. Bell *et al.*, *Phys. Rev. Lett.* **95**, 151802 (2005).
52. S. Davidson, M. Gorbahn and A. Santamaria, *Phys. Lett.* **B626**, 151 (2005).
53. N. F. Bell *et al.*, Phys. Lett. to be published; hep-ph/0606248.